Cancer Cell
Article

Stabilization of N-Myc Is a Critical Function of Aurora A in Human Neuroblastoma

Tobias Otto,[1] Sebastian Horn,[1] Markus Brockmann,[1] Ursula Eilers,[1] Lars Schüttrumpf,[1] Nikita Popov,[1] Anna Marie Kenney,[2] Johannes H. Schulte,[3] Roderick Beijersbergen,[4] Holger Christiansen,[5] Bernd Berwanger,[5,6] and Martin Eilers[1,6,7,*]

[1]Institute of Molecular Biology and Tumor Research, Emil-Mannkopf-Straße 2, 35037 Marburg, Germany
[2]Cancer Biology and Genetics, Memorial Sloan-Kettering Cancer Center, New York, NY 10021, USA
[3]Department of Pediatric Hematology, Oncology and Endocrinology, University Hospital of Essen, 45122 Essen, Germany
[4]Netherlands Cancer Center, Plesmanlaan 121, Amsterdam CX 1066, The Netherlands
[5]Children's Hospital, Medical Center, Philipps-Universität Marburg, Baldingerstraße, 35043 Marburg, Germany
[6]These authors contributed equally to this work
[7]Present address: Department of Physiological Chemistry, Biocenter, Universität Würzburg, Am Hubland, 97074 Würzburg, Germany
*Correspondence: martin.eilers@biozentrum.uni-wuerzburg.de
DOI 10.1016/j.ccr.2008.12.005

SUMMARY

In human neuroblastoma, amplification of the *MYCN* gene predicts poor prognosis and resistance to therapy. In a shRNA screen of genes that are highly expressed in *MYCN*-amplified tumors, we have identified *AURKA* as a gene that is required for the growth of *MYCN*-amplified neuroblastoma cells but largely dispensable for cells lacking amplified *MYCN*. Aurora A has a critical function in regulating turnover of the N-Myc protein. Degradation of N-Myc requires sequential phosphorylation by cyclin B/Cdk1 and Gsk3. N-Myc is therefore degraded during mitosis in response to low levels of PI3-kinase activity. Aurora A interacts with both N-Myc and the SCF^{Fbxw7} ubiquitin ligase that ubiquitinates N-Myc and counteracts degradation of N-Myc, thereby uncoupling N-Myc stability from growth factor-dependent signals.

INTRODUCTION

Human neuroblastoma is a tumor of the peripheral sympathetic nervous system that is derived from highly proliferative migratory cells of the neural crest. During normal development, these neuroblasts undergo cell-cycle exit and differentiation when they colonize ganglia and spinal cord areas (Grimmer and Weiss, 2006). One characteristic feature of neuroblastoma is a strongly varying course of the disease that ranges from spontaneous regression to progressive disease and metastasis (Westermann and Schwab, 2002). A factor that predicts poor prognosis is amplification of the *MYCN* gene, which disrupts the cell-cycle exit and terminal differentiation that occurs during normal neuroblast development (Grimmer and Weiss, 2006). Consistent with this view, ectopic expression of *MYCN* can suppress differentiation of neuroblastoma cells in culture.

Transgenic models have demonstrated that Myc-induced tumors remain dependent on Myc after they have been established, arguing that strategies that interfere with Myc function may have significant therapeutic value (Arvanitis and Felsher, 2006). Similarly, a number of experimental strategies suggest that *MYCN*-amplified neuroblastoma cells are addicted to high levels of N-Myc, at least in tissue culture (Galderisi et al., 1999).

Neuroblastomas with amplified *MYCN* have a characteristic gene expression profile (Berwanger et al., 2002). We speculated that genes that are expressed in a *MYCN*-dependent manner might be required specifically for the growth of *MYCN*-amplified neuroblastomas for one of two reasons. First, tumors that depend on high levels of N-Myc may also depend on specific upstream regulatory factors or downstream target genes of N-Myc that are less essential for the growth of N-Myc-independent tumors. For example, mice carrying only a single copy of the gene encoding ornithine decarboxylase (*ODC1*), a target gene of Myc, have no detectable phenotype yet are resistant to Myc-induced lymphomagenesis (Nilsson et al., 2005). Second, high levels of Myc proteins induce apoptosis, and a specific pattern of gene expression may therefore be required to suppress

SIGNIFICANCE

AURKA is an oncogene that is amplified in many human tumors, and the encoded kinase Aurora A is a target for current drug development. Here we identify Aurora A as a protein that binds to and stabilizes N-Myc. We suggest that Aurora A-mediated stabilization of N-Myc contributes to the development of neuroblastoma since it interferes with the cell-cycle exit of neuroblasts in developing peripheral neurons. This function is critical for the growth of *MYCN*-amplified neuroblastoma cells and is likely to be important for other *MYCN*-associated tumors. Aurora A stabilizes N-Myc independently of its kinase activity. Thus, inhibition of Aurora A activity using small molecules may fail to block a critical oncogenic function of Aurora A.

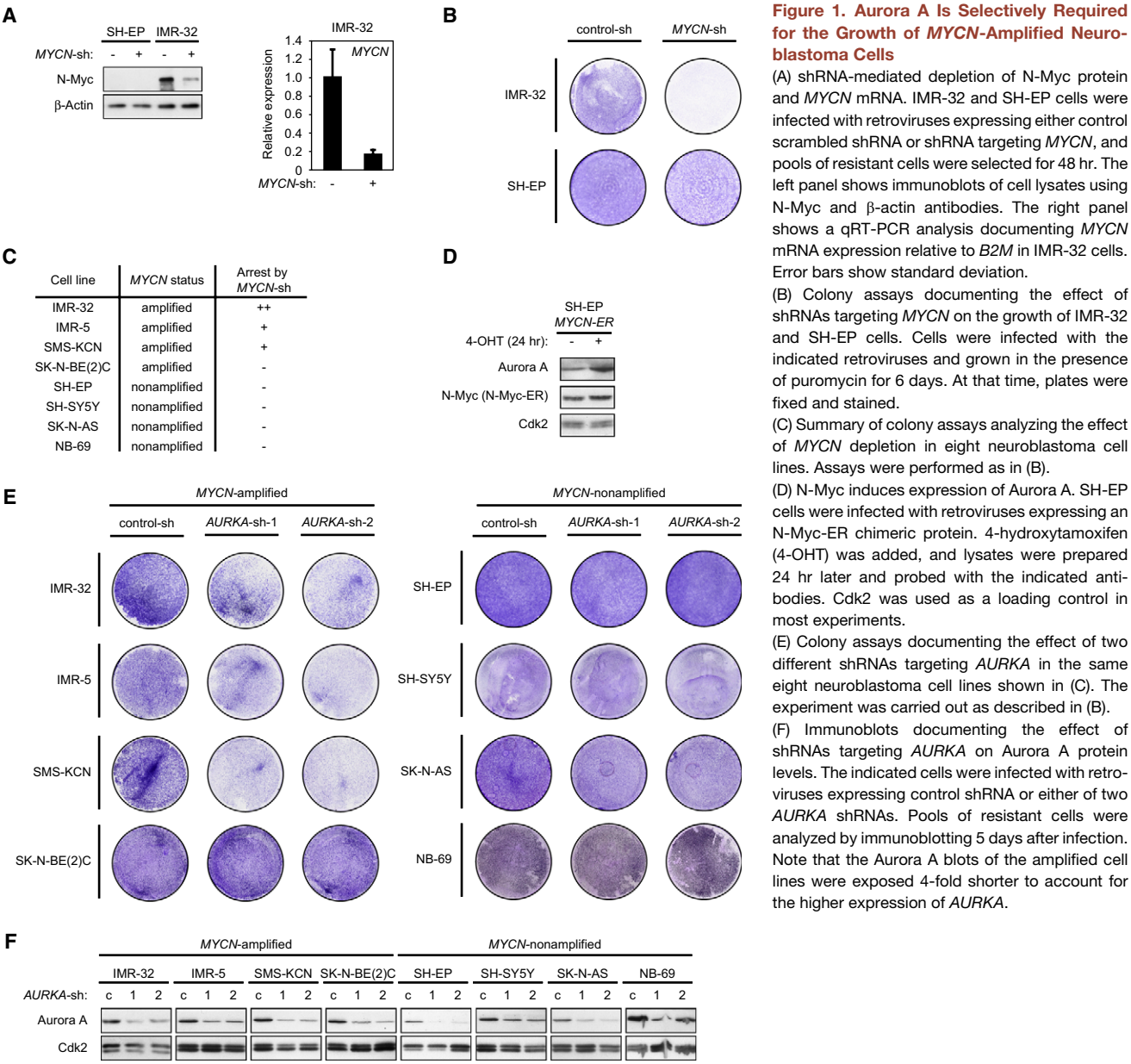

Figure 1. Aurora A Is Selectively Required for the Growth of *MYCN*-Amplified Neuroblastoma Cells

(A) shRNA-mediated depletion of N-Myc protein and *MYCN* mRNA. IMR-32 and SH-EP cells were infected with retroviruses expressing either control scrambled shRNA or shRNA targeting *MYCN*, and pools of resistant cells were selected for 48 hr. The left panel shows immunoblots of cell lysates using N-Myc and β-actin antibodies. The right panel shows a qRT-PCR analysis documenting *MYCN* mRNA expression relative to *B2M* in IMR-32 cells. Error bars show standard deviation.

(B) Colony assays documenting the effect of shRNAs targeting *MYCN* on the growth of IMR-32 and SH-EP cells. Cells were infected with the indicated retroviruses and grown in the presence of puromycin for 6 days. At that time, plates were fixed and stained.

(C) Summary of colony assays analyzing the effect of *MYCN* depletion in eight neuroblastoma cell lines. Assays were performed as in (B).

(D) N-Myc induces expression of Aurora A. SH-EP cells were infected with retroviruses expressing an N-Myc-ER chimeric protein. 4-hydroxytamoxifen (4-OHT) was added, and lysates were prepared 24 hr later and probed with the indicated antibodies. Cdk2 was used as a loading control in most experiments.

(E) Colony assays documenting the effect of two different shRNAs targeting *AURKA* in the same eight neuroblastoma cell lines shown in (C). The experiment was carried out as described in (B).

(F) Immunoblots documenting the effect of shRNAs targeting *AURKA* on Aurora A protein levels. The indicated cells were infected with retroviruses expressing control shRNA or either of two *AURKA* shRNAs. Pools of resistant cells were analyzed by immunoblotting 5 days after infection. Note that the Aurora A blots of the amplified cell lines were exposed 4-fold shorter to account for the higher expression of *AURKA*.

apoptosis (Valsesia-Wittmann et al., 2004). In this manner, *MYCN*-amplified neuroblastomas might depend not only on N-Myc itself but also on individual genes that are contained in their expression profile. If so, inhibition of such genes might uncover "synthetic lethal" effects that allow selective interference with the growth of *MYCN*-amplified neuroblastomas (Kaelin, 2005). To identify possible synthetic lethal interactions, we performed a shRNA screen analyzing 194 genes that are expressed in a manner dependent on amplified *MYCN* in human neuroblastoma or that are known to be direct target genes of Myc.

RESULTS

To determine whether *MYCN*-amplified neuroblastoma cells depend on N-Myc, we designed retroviral shRNA vectors targeting *MYCN* and tested them initially in IMR-32 cells, which have amplified *MYCN*, and SH-EP cells, which have a single-copy, silenced *MYCN* gene (Figure 1A). Both cell lines were stably transfected with plasmids expressing the ecotropic retroviral receptor and a hygromycin resistance gene, and pools of resistant cells were used in the subsequent experiments. shRNA vectors targeting *MYCN* led to a reduction in *MYCN* mRNA and in N-Myc protein levels in IMR-32 cells, whereas no N-Myc protein was detectable in SH-EP cells (Figure 1A). Knockdown of *MYCN* led to a strong reduction in colony formation of IMR-32 cells, but not of SH-EP cells (Figure 1B). Fluorescence-activated cell sorting (FACS) analysis showed that depletion of *MYCN* delayed progression of IMR-32 cells through the cell cycle but did not induce apoptosis (see Figure S1 available online). shRNAs targeting *MYCN* inhibited proliferation of three out of four

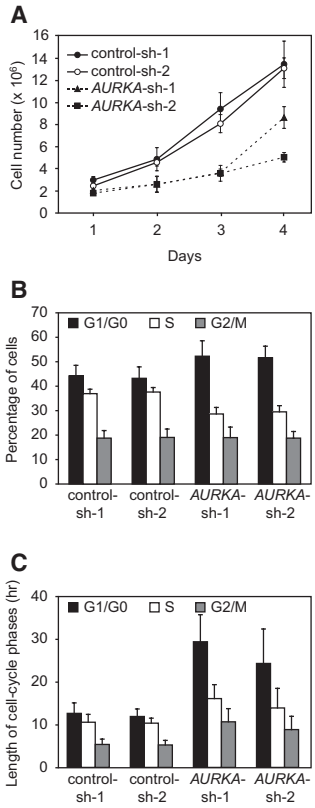

Figure 2. Aurora A Is Required for Cell-Cycle Progression of *MYCN*-Amplified Neuroblastoma Cells

(A) Growth curve of IMR-32 cells infected with two control shRNAs (scrambled-sh and GFP-sh) or two shRNAs targeting *AURKA*. IMR-32 cells were infected with the indicated retroviruses and selected. Counting was begun 3 days after infection (day 1 in graph). For each day and each shRNA, three plates were counted and averaged. Error bars show standard deviation of triplicate samples.

(B) Summary of FACS analysis documenting the effects of Aurora A depletion on cell cycle in IMR-32 cells. Cells were infected as before, and resistant cell pools were harvested during exponential growth in 10% FBS. For each condition, the cell-cycle distribution of triplicate samples after staining with propidium iodide was measured at days 1, 2, and 3, and all nine samples were averaged. Error bars show standard deviation. No significant number of sub-G1 cells was detected in any condition.

(C) Effect of Aurora A depletion on length of cell-cycle phases. The data obtained in (A) and those obtained from the FACS analysis in (B) were combined to calculate the length of each phase of the cell cycle of IMR-32 cells. Error bars show standard deviation calculated via the Gaussian error propagation law.

MYCN-amplified cells tested, the exception being SK-N-BE(2)C cells (Figure 1C). In contrast, none of four neuroblastoma lines lacking amplified *MYCN* depended on expression of N-Myc. In addition, a pool of three additional vectors expressing shRNAs targeting *MYCN* reduced the rate of proliferation of IMR-32 relative to SH-EP cells (Table S1). In contrast, control scrambled shRNA vectors did not affect the relative rate of proliferation of IMR-32 versus SH-EP cells. This demonstrates that the majority of *MYCN*-amplified cell lines, but not neuroblastoma cells lacking amplified *MYCN*, depend on N-Myc for proliferation.

In order to identify additional genes selectively required for the growth of *MYCN*-amplified neuroblastoma cells, we selected 194 genes on the basis of two criteria: First, we selected all 67 genes that we had previously found to be expressed at an enhanced level in *MYCN*-amplified primary neuroblastomas (Berwanger et al., 2002). Second, we used a public database (www.myc-cancer-gene.org) to extract all genes known to be direct targets of Myc (for which binding of Myc to the promoter had been demonstrated) and that are induced by Myc. At the time we started these experiments, these were additional 127 genes (Table S1). For each gene, three retroviral shRNA vectors were either picked from a preexisting library (Berns et al., 2004) (61 genes) or cloned from oligonucleotides (133 genes) and pooled before transfection of Phoenix-Eco packaging cells. Control experiments using ten randomly picked shRNA pools showed that both cell lines displayed similar knockdown efficiencies for each pool. Specifically, 60% of the shRNA pools used resulted in a significant (2-fold or more) knockdown of their target gene in both cell lines (data not shown).

Subsequently, we infected both IMR-32 and SH-EP cells with each of the 194 pools of shRNA vectors, selected resistant cells, and estimated a proliferation rate of cell pools from plates stained at a fixed time point after infection. Using a reduction in growth rate similar to or better than the *MYCN* shRNA pool as cutoff, the experiment identified a group of 17 genes that, when inhibited with shRNA, reproducibly inhibited the growth of IMR-32 cells but had no or little effect on SH-EP cells (Table S1). We focused on Aurora A in the subsequent analysis since the gene encoding Aurora A (*AURKA*) is amplified in a subset of human neuroblastomas, providing genetic evidence for a selective pressure for enhanced Aurora A levels in this tumor (Zhou et al., 1998). Previous microarray analyses have demonstrated elevated levels of *AURKA* mRNA in *MYCN*-amplified relative to nonamplified primary neuroblastomas, suggesting that high levels of N-Myc directly or indirectly enhance expression of *AURKA* mRNA (e.g., Berwanger et al., 2002). We confirmed these findings by analyzing Aurora A protein and *AURKA* mRNA expression in multiple primary neuroblastomas (Figure S2). Furthermore, activation of a conditional allele of *MYCN* (*MYCN-ER*) (Schulte et al., 2008) in SH-EP cells induced expression of Aurora A protein and *AURKA* mRNA even in exponentially proliferating cells (Figure 1D and data not shown).

We tested two different shRNAs targeting *AURKA* (*AURKA*-sh) in the same eight neuroblastoma cell lines that had been tested for dependence on N-Myc. We found that expression of *AURKA*-sh inhibited proliferation of the same three *MYCN*-amplified neuroblastoma cell lines that depend on high N-Myc protein levels for proliferation, but none of the cell lines that do not depend on N-Myc (Figure 1E). Both shRNAs led to a 3- to 4-fold reduction in *AURKA* mRNA and Aurora A protein levels in most of the cell lines, with minor variations (Figure 1F and data not shown). Therefore, the differential effect on cell proliferation is not due to different knockdown efficiencies. Five additional *AURKA*-sh vectors that led to only a small or no reduction in *AURKA* mRNA levels had no effect on the proliferation of either IMR-32 or SH-EP cells, demonstrating a close correlation between knockdown efficiency and biological effect (data not shown).

Growth curves showed that expression of *AURKA*-sh inhibited the exponential growth of IMR-32 cells (Figure 2A), but not of SH-EP cells (data not shown). FACS analysis revealed that

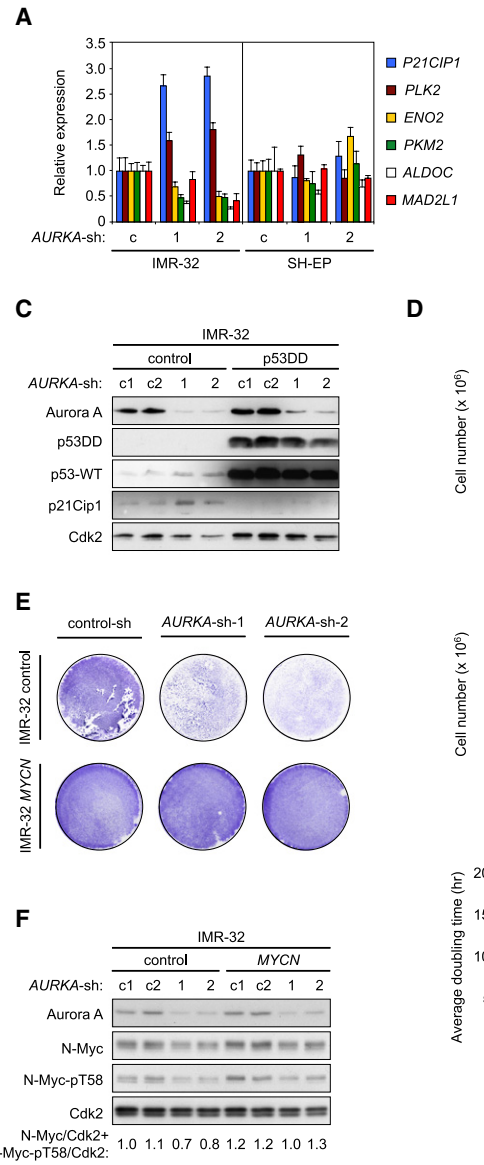

Figure 3. Molecular Analysis of Aurora A Depletion in *MYCN*-Amplified Neuroblastoma Cells

(A) qRT-PCR analysis documenting selective upregulation of two p53 target genes (*P21CIP1* and *PLK2*), three glycolytic genes (*ENO2*, *PKM2*, and *ALDOC*), and the cell-cycle gene *MAD2L1* in IMR-32 cells, but not in SH-EP cells. Note that *MAD2L1* is a direct target gene of N-Myc (Berwanger et al., 2002). Error bars indicate standard deviation.

(B) Immunoblots documenting protein levels of N-Myc, p53, p21Cip1, and Aurora A in pools of IMR-32 cells infected with retroviruses expressing either control shRNA or two different shRNAs targeting *AURKA*.

(C) A dominant-negative allele of p53 (p53DD) abrogates induction of p21Cip1 in response to Aurora A depletion. IMR-32 cells were infected with either empty vector (control) retroviruses or retroviruses expressing p53DD. Resistant clones were superinfected with retroviruses expressing either control shRNA or two different shRNAs targeting *AURKA*. The panels show immunoblots using the indicated antibodies in pools of resistant cells.

(D) Expression of p53DD does not relieve inhibition of proliferation by depletion of Aurora A. The upper two panels show growth curves of IMR-32 cells infected with the indicated retroviruses. Error bars indicate standard deviation. The lower panel shows doubling times calculated from these curves (averaged for control shRNA and shRNAs targeting *AURKA*).

(E) Colony assays documenting the effect of depletion of Aurora A on IMR-32 cells and on IMR-32 cells superinfected with retroviruses expressing *MYCN*.

(F) Immunoblots documenting expression of Aurora A, N-Myc, and N-Myc phosphorylated at T58 in IMR-32 cells infected with the indicated viruses. Numbers at bottom indicate the ratio of N-Myc expression (averaged from the N-Myc and the N-Myc-pT58 blots) to expression of Cdk2.

depletion of Aurora A did not induce apoptosis but led to an increase in the percentage of cells in the G1 phase of the cell cycle and a concomitant decrease in the number of cells in S phase (Figure 2B). We used the growth curves to estimate doubling times and combined both pieces of information to calculate the length of each phase of the cell cycle (Figure 2C). We concluded that depletion of Aurora A led to an increase in length of all phases of the cell cycle of IMR-32 cells, with the effect being strongest for the G1 phase. Therefore, the effect of Aurora A depletion in *MYCN*-amplified cells is not restricted to the G2/M phase, when the kinase activity of Aurora A is highest (Hirota et al., 2003).

In order to identify potential effectors that might cause this phenotype, we performed a microarray analysis of IMR-32 cells expressing either control scrambled shRNA or shRNAs targeting *AURKA*. The analysis showed that depletion of Aurora A affected expression of many genes. Gene set enrichment analysis (GSEA) (Subramanian et al., 2005) and Ingenuity Pathways Analysis (www.ingenuity.com) revealed a close similarity between the genes induced upon depletion of Aurora A and genes induced by genotoxic stress. Examples are the cell-cycle inhibitor p21Cip1 (*P21CIP1*) and polo-like kinase 2 (*PLK2*) (Figure 3A; Figure S3A). Furthermore, the analysis showed that the set of genes downregulated upon depletion of Aurora A was enriched in genes encoding glycolytic enzymes (shown for enolase 2 [*ENO2*], pyruvate kinase M2 [*PKM2*], and aldolase [*ALDOC*] in Figure 3A) and in cell-cycle proteins (shown for *MAD2L1*), functions that have been associated with target genes of Myc. Comparison with the database of Myc target genes confirmed that depletion of Aurora A reduced expression of many such genes (Figure S3B). qRT-PCR analysis showed that both responses were more prominent in IMR-32 cells since depletion of Aurora A had little effect on expression of these genes in SH-EP cells (Figure 3A).

Upregulation of *P21CIP1* in response to genotoxic stress is mediated by p53, suggesting that depletion of Aurora A might activate the function of p53. Indeed, Aurora A phosphorylates p53 and promotes its nuclear export and degradation (Katayama et al., 2004). Therefore, high levels of Aurora A might be required to restrict the function of p53 in the presence of elevated levels of N-Myc. Consistent with this view, immunoblots showed that

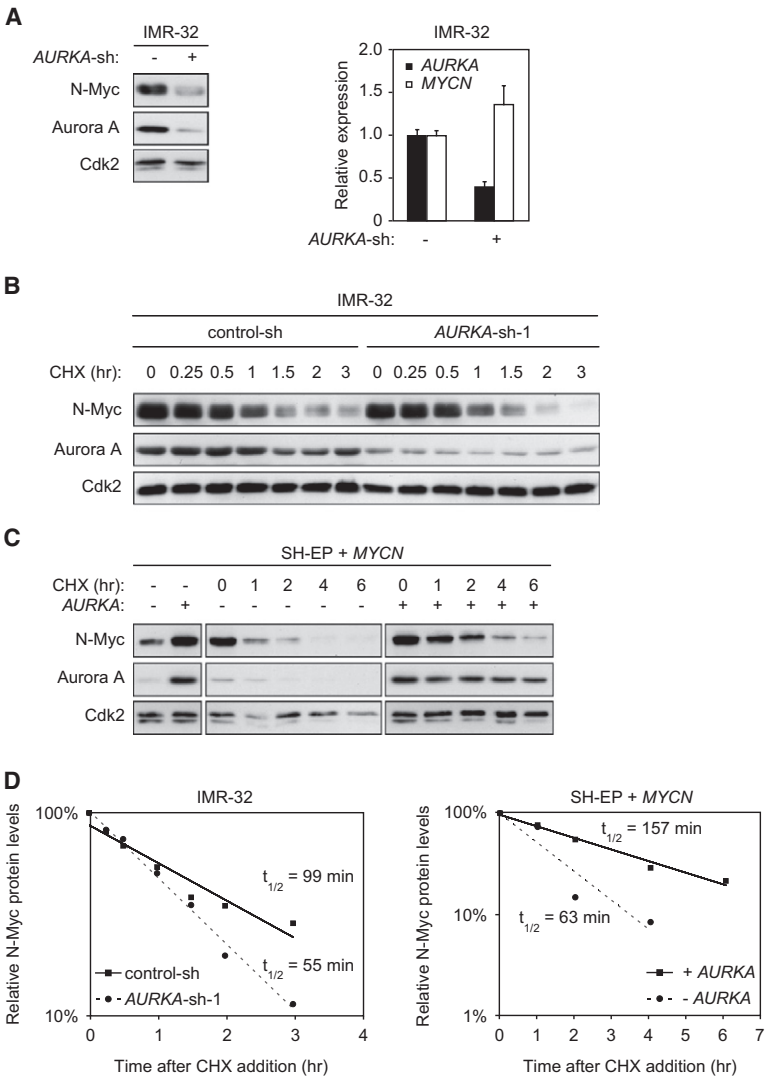

Figure 4. Aurora A Regulates N-Myc Protein Stability

(A) Immunoblots documenting steady-state levels of N-Myc and Aurora A protein (left panel) and qRT-PCR analysis documenting levels of *AURKA* and *MYCN* mRNAs (right panel) in IMR-32 cells infected with either control shRNA or *AURKA*-sh-2. Error bars show standard deviation.

(B) Immunoblots documenting the stability of N-Myc in IMR-32 cells expressing either control shRNA or shRNA targeting *AURKA*. At the start of the experiment, cells were treated with cycloheximide (CHX). Lysates were prepared at the indicated times after addition of CHX and probed with the indicated antibodies.

(C) Stabilization of N-Myc by expression of Aurora A. SH-EP cells were cotransfected with CMV-driven vectors expressing *MYCN* and *AURKA* as indicated. The leftmost two lanes document steady-state levels of N-Myc and Aurora A 48 hr after transfection. qRT-PCR analysis showed that Aurora A did not affect the *MYCN* mRNA levels in this experiment (data not shown). Subsequently, CHX was added to cells, and lysates were prepared at the indicated times after addition of CHX and analyzed by immunoblotting. Note that the exposure time of the upper middle panel documenting stability of N-Myc in the absence of Aurora A is 4-fold longer than the other panels to equalize the signal at the 0 hr time point.

(D) Quantification of stability assays. The left panel shows a quantification of the results shown in (B); the right panel shows a quantification of the results shown in (C). Levels of N-Myc are normalized to Cdk2.

depletion of Aurora A elevated both p21Cip1 and p53 protein levels (Figure 3B). Cells depleted of Aurora A also showed a decrease in levels of N-Myc protein, which could account for the reduced expression of Myc target genes (Figure 3B). Furthermore, N-Myc repressed expression of p21Cip1 (Figure S4A). As a consequence, a reduction in N-Myc levels may contribute to upregulation of *P21CIP1* mRNA levels.

To test whether induction of p53 mediates the effect of *AURKA*-sh on the proliferation of IMR-32 cells, we expressed a carboxy-terminal fragment of p53, p53DD, which acts in a dominant-negative manner (Gottlieb et al., 1994). We then superinfected these cells with retroviruses expressing *AURKA*-sh (Figure 3C). Expression of p53DD abrogated induction of p21Cip1 and led to constitutively elevated expression of endogenous p53, indicative of repression of *MDM2*. p53DD caused a moderate reduction in the growth rate of IMR-32 cells but did not relieve the inhibition of proliferation caused by depletion of Aurora A (Figure 3D). FACS analysis showed that the arrest in response to Aurora A depletion was shifted toward the G2/M phase in IMR-32/p53DD cells, consistent with the reduced p21Cip1 expression (Figure S4B). In contrast, moderate elevation of N-Myc levels using recombinant retroviruses alleviated the suppression of colony formation by *AURKA*-sh (Figures 3E and 3F), indicating that the reduction in N-Myc levels is the critical mechanism by which depletion of Aurora A inhibits proliferation. In support of this notion, expression of *AURKA*-sh caused a reduction in N-Myc expression in three additional *MYCN*-amplified cell lines tested (Figure S5A). In contrast, effects on p53 were not consistent between these four cell lines (data not shown). Finally, depletion of Aurora A had no effect on steady-state levels of c-Myc (data not shown), providing an explanation for the observed specificity of dependence on Aurora A.

Depletion of Aurora A in IMR-32 cells reduced the steady-state levels of N-Myc protein but led to a slight increase in *MYCN* mRNA levels (Figure 4A), arguing that Aurora A regulates N-Myc levels via a posttranscriptional mechanism. Indeed, depletion of Aurora A led to an increased turnover of N-Myc protein, which became apparent when IMR-32 cells were treated with cycloheximide to block new protein synthesis and cells were harvested at different time points afterwards (Figure 4B); under these conditions, depletion of Aurora A reduced the half-life of endogenous N-Myc from 99 to 55 min (Figure 4D). Conversely, coexpression of Aurora A strongly enhanced steady-state levels of N-Myc upon transient transfection of CMV-driven expression vectors in SH-EP cells, and this corresponded to an increase in N-Myc stability (Figures 4C and 4D); pulse-chase experiments using ^{35}S labeling confirmed this result (Figure S5B). We concluded that Aurora A stabilizes the N-Myc protein.

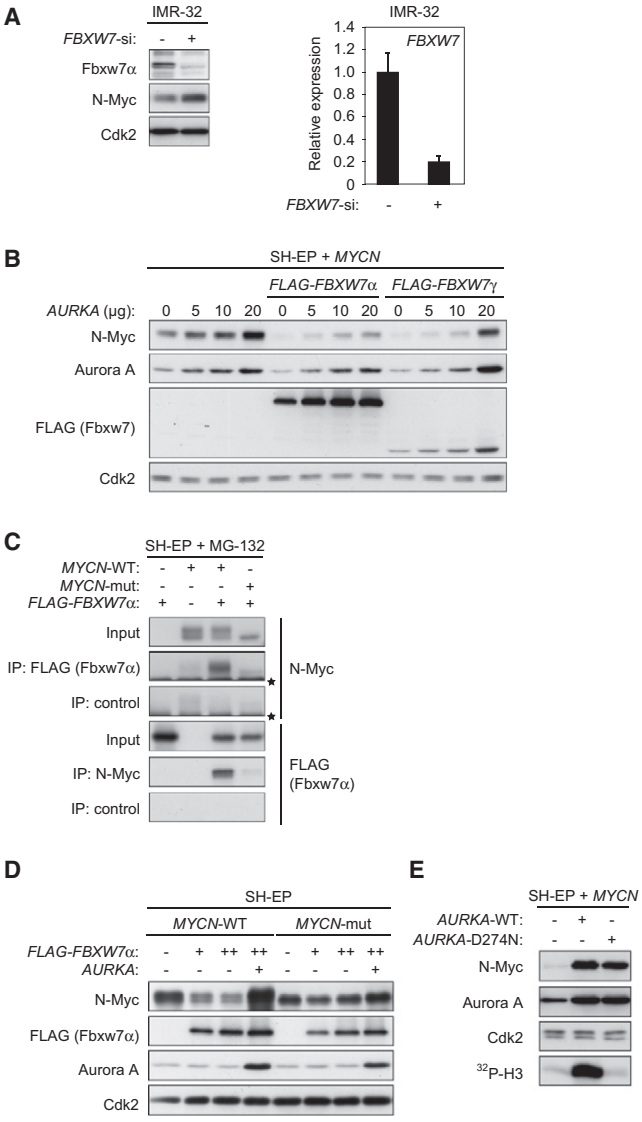

Figure 5. Aurora A Stabilizes N-Myc by Counteracting Fbxw7-Mediated Degradation

(A) Depletion of *FBXW7* enhances steady-state levels of N-Myc. IMR-32 cells were infected with control shRNA vectors or with shRNA targeting *FBXW7*. After selection, cells were harvested and immunoblots were probed with antibodies against Fbxw7 and N-Myc (left panel). In parallel, *FBXW7* mRNA levels were determined relative to *RPS14* (right panel). Error bars show standard deviation.

(B) Aurora A inhibits Fbxw7-mediated degradation of N-Myc. SH-EP cells were transfected with CMV-driven expression vectors encoding N-Myc, Aurora A, and FLAG-tagged Fbxw7α or Fbxw7γ as indicated. Forty-eight hours after transfection, cells were lysed and immunoblots were probed with N-Myc or FLAG antibodies. The numbers refer to the amount (in μg) of plasmid that was transfected.

(C) Fbxw7α binds to wild-type N-Myc via T58 and S62. SH-EP cells were transfected with CMV-driven expression vectors encoding either wild-type N-Myc (*MYCN*-WT) or N-Myc(T58A;S62A) (*MYCN*-mut) and FLAG-tagged Fbxw7α as indicated. Forty-eight hours after transfection, cells were lysed and lysates were immunoprecipitated with N-Myc, FLAG, or control antibodies. Input lanes correspond to 5% of the material used for immunoprecipitations. To block proteasomal degradation, the proteasome inhibitor MG-132 was added to the cells 4 hr before harvesting. Asterisk denotes the IgG heavy chain.

(D) The effects of both Fbxw7 and Aurora A are specific for wild-type N-Myc. SH-EP cells were transfected with vectors encoding FLAG-tagged Fbxw7α, Aurora A, and either wild-type N-Myc or N-Myc(T58A;S62A); + and ++ reflect the amount of transfected plasmid. Forty-eight hours after transfection, cells were lysed and immunoblots were probed with the indicated antibodies.

(E) Stabilization of N-Myc by Aurora A is independent of kinase activity. SH-EP cells were transfected with CMV-driven expression vectors encoding either wild-type Aurora A or Aurora A(D274N). Forty-eight hours after transfection, cells were lysed. An aliquot of the lysates was used for immunoblotting as shown in the top three rows. A second aliquot was used for immunocomplex kinase assays using Aurora A antibody and histone H3 as substrate. Controls established that Aurora A(D274N) was immunoprecipitated as efficiently as wild-type Aurora A (data not shown). The bottom row shows an autoradiogram documenting the incorporation of [^{32}P]phosphate into histone H3 in this assay.

In neuronal progenitor cells, degradation of N-Myc requires phosphorylation of threonine 58 (T58) by Gsk3 (Sjostrom et al., 2005). The surrounding sequence (Mycbox I) is identical to that in c-Myc, and the corresponding residue in c-Myc is recognized by the SCF^{Fbxw7} ubiquitin ligase, suggesting that degradation of N-Myc is carried out by the same complex (Yada et al., 2004). Consistent with this view, depletion of Fbxw7 led to an accumulation of N-Myc in IMR-32 cells (Figure 5A). Conversely, expression of either the nuclear or the nucleolar isoform of Fbxw7 (Fbxw7α or Fbxw7γ; Welcker et al., 2004) led to a strong decrease in N-Myc protein levels upon cotransfection in SH-EP cells (Figure 5B). Coexpression of increasing amounts of *AURKA* abolished the Fbxw7-mediated decrease in N-Myc levels. In both N-Myc and c-Myc, phosphorylation of T58 by Gsk3 requires a priming phosphorylation at serine 62 (S62); mutation of both residues in c-Myc abolishes the interaction with SCF^{Fbxw7} (Yada et al., 2004). To test whether stabilization of N-Myc by Aurora A is mediated by inhibition of SCF^{Fbxw7}, we generated a mutant allele of N-Myc in which both T58 and S62 are replaced by alanine (*MYCN*-mut). Mutation of both residues strongly attenuated the interaction of N-Myc with Fbxw7 (Figure 5C). Consistently, expression of Fbxw7α strongly reduced steady-state levels of wild-type N-Myc, and this was reversed by coexpression of Aurora A; in contrast, neither Fbxw7α nor Aurora A had a significant effect on levels of the mutant N-Myc protein (Figure 5D). We concluded that stabilization of N-Myc by Aurora A occurs via inhibition of SCF^{Fbxw7}-mediated degradation.

We considered several models of how Aurora A might affect degradation of N-Myc by SCF^{Fbxw7}. To test whether phosphorylation of either Fbxw7 or N-Myc is required for this effect, we generated a total of eight different mutant alleles of *AURKA*, all of which have previously been reported to be deficient in kinase activity. With a single exception (*AURKA*-S342D, which was expressed at lower levels than the other alleles), each mutant was as capable as wild-type Aurora A in stabilizing N-Myc upon transient transfection into SH-EP cells (Figure 5E; Figure S6A). We confirmed that one of these alleles, D274N, is unable to phosphorylate recombinant histone H3 in vitro (Figure 5E). Furthermore, treatment of transfected cells with hesperadin, an inhibitor of Aurora kinases, abolished phosphorylation of histone H3 but had no effect on stabilization of N-Myc by Aurora A (Figure S6B) (Hauf et al., 2003). Finally, treatment of IMR-32 cells with hesperadin had no effect on endogenous N-Myc levels

under conditions wherein autophosphorylation of Aurora A was significantly diminished (data not shown). Taken together, these data show that stabilization of N-Myc is independent of Aurora A kinase activity.

We therefore considered the possibility that Aurora A forms a complex with either Fbxw7 or N-Myc in vivo to prevent degradation of N-Myc. Consistent with this suggestion, immunoprecipitation experiments revealed that Aurora A was present in Fbxw7α immunoprecipitates when both proteins were expressed in SH-EP cells and vice versa, suggesting that both proteins can form a stable complex in vivo (Figure 6A). Since Aurora A itself can be a substrate for Fbxw7-mediated ubiquitination and subsequent degradation, we considered the possibility that elevated levels of Aurora A compete with N-Myc for access to Fbxw7 (Fujii et al., 2006). We therefore tested whether increasing amounts of Aurora A displace N-Myc from binding to Fbxw7. However, expression even of high amounts of *AURKA* did not displace N-Myc from a complex with Fbxw7α when all three proteins were coexpressed by transient transfection in SH-EP cells (Figure 6B). Furthermore, expression of *AURKA* had no effect on Fbxw7-mediated degradation of cyclin E (Figure 6C) and c-Myc (data not shown), two additional substrates of Fbxw7, further arguing that stabilization is not mediated by competition among substrates of Fbxw7 (Koepp et al., 2001).

Alternatively, Aurora A might interact with N-Myc that is bound to Fbxw7 and inhibit its degradation. To test this notion, we cotransfected expression vectors encoding Aurora A and N-Myc into SH-EP cells and immunoprecipitated lysates with either control antibodies or antibodies directed against either protein (Figure 6D). Immunoblots revealed that Aurora A was present in N-Myc immunoprecipitates and vice versa (Figure 6D). Furthermore, immunoprecipitations from lysates of IMR-32 cells revealed the presence of endogenous Aurora A in N-Myc immunoprecipitates, demonstrating that the endogenous proteins interact with each other; addition of nocodazole to arrest cells in mitosis did not enhance the interaction, arguing that the interaction is not restricted to mitotic cells (Figure 6E). Aurora A and N-Myc interacted both in the presence (Figure 6E) and in the absence (Figure 6F) of a proteasome inhibitor, demonstrating that the interaction is not due to the accumulation of partially unfolded proteins when the function of the proteasome is inhibited.

Endogenous N-Myc was present in Fbxw7 immunoprecipitates from IMR-32 cells (Figure S6C). Importantly, N-Myc mutated at T58 and S62 (*MYCN*-mut) showed a reduction in its interaction with Aurora A that mirrored the reduced interaction with Fbxw7 (Figure 6G). We concluded that Aurora A interacts preferentially or exclusively with N-Myc that is bound to SCF^{Fbxw7}.

Degradation of Myc proteins occurs in a stepwise process, and distinct sequence elements are required for ubiquitination of Myc and for degradation of ubiquitinated Myc proteins (Herbst et al., 2004). We therefore tested whether Aurora A interferes with Fbxw7-mediated ubiquitination of N-Myc or with the subsequent degradation of ubiquitinated N-Myc. Transfection of SH-EP cells with expression vectors encoding N-Myc and His-tagged ubiquitin showed that N-Myc was strongly ubiquitinated. Expression of Aurora A led to an accumulation of ubiquitinated N-Myc that paralleled or exceeded the increase in N-Myc levels, demonstrating that Aurora A acts at a postubiquitination step to stabilize N-Myc (Figure 6H). As expected, the ubiquitination of N-Myc mutated at T58 and S62 was significantly reduced relative to wild-type N-Myc, and Aurora A had little effect on ubiquitination of *MYCN*-mut (Figure S7A). Indeed, direct measurements of the stability of ubiquitinated forms of N-Myc using cycloheximide showed that expression of Aurora A inhibited the turnover of ubiquitinated N-Myc (Figure S7B). Importantly, Aurora A induced the accumulation of ubiquitinated N-Myc in the presence of wild-type ubiquitin and in the presence of ubiquitin in which K48 was replaced by arginine (K48R; Figure S7C). In contrast, total levels of ubiquitination of N-Myc were strongly reduced in the presence of a mutant ubiquitin in which all lysines except K48 were mutated to arginine (K48-only), and Aurora A failed to stabilize N-Myc under these conditions (Figure 6I, left panel); this effect was specific for N-Myc since K48-only ubiquitin supported ubiquitination of cyclin E as efficiently as wild-type ubiquitin (Figure 6I, right panel). We concluded that Aurora A stabilizes N-Myc by promoting the accumulation of ubiquitin chains with linkages other than K48 that are degraded less efficiently by the proteasome (Kim et al., 2007). Furthermore, mutation of K63 of wild-type ubiquitin to arginine did not abolish the ability of Aurora A to stabilize N-Myc, arguing that linkage via K63 is not strictly required for stabilization by Aurora A (Figure S7C). Consistent with this suggestion, restoration of either K63 or K11 into K48-only ubiquitin (generating K48/63 and K48/11 ubiquitin) partially restored the ability of Aurora A to induce the accumulation of ubiquitinated N-Myc, arguing that chains linked via either residue can mediate stabilization of N-Myc (Figure S7D).

In neuronal progenitor cells, S62 in N-Myc is phosphorylated by cyclin B/Cdk1 complexes, suggesting that Aurora A might stabilize N-Myc in the G2/M phase of the cell cycle (Sjostrom et al., 2005). Consistently, levels of both Aurora A and N-Myc increased when synchronized IMR-32 cells entered G2 (Figure S8A); also, Aurora A and N-Myc colocalized in mitotic cells (Figure S8B). Furthermore, accumulation of cells in mitosis using the spindle poison nocodazole led to a time-dependent accumulation of N-Myc phosphorylated at S62 in IMR-32 cells, both in the absence and in the presence of the proteasome inhibitor MG-132 (Figure 7A). As shown before, transient expression of Aurora A led to an accumulation of N-Myc in SH-EP cells (Figure 7B). N-Myc that accumulated under these conditions was phosphorylated at both T58 and S62. In order to promote phosphorylation of endogenous N-Myc at T58 and S62, we used nocodazole and LY294002, an inhibitor of PI3-kinase. Since Gsk3 is phosphorylated and inhibited by Akt, which is downstream of PI3-kinase, addition of LY294002 activates Gsk3 (Cross et al., 1995). In contrast to what has been observed in neuronal progenitor cells, addition of nocodazole and LY294002 had an only weakly additive effect on steady-state levels of N-Myc in two *MYCN*-amplified neuroblastoma cell lines (Figure 7C). By itself, depletion of Aurora A reduced levels of N-Myc protein 2-fold, as observed before. Depletion of Aurora A synergized with the inhibitors in reducing steady-state levels of N-Myc, and the combination of all three treatments all but eliminated N-Myc in both cell lines. Together, these data demonstrate directly that high levels of Aurora A in *MYCN*-amplified neuroblastoma cells interfere with the PI3-kinase-dependent and mitosis-specific degradation of N-Myc.

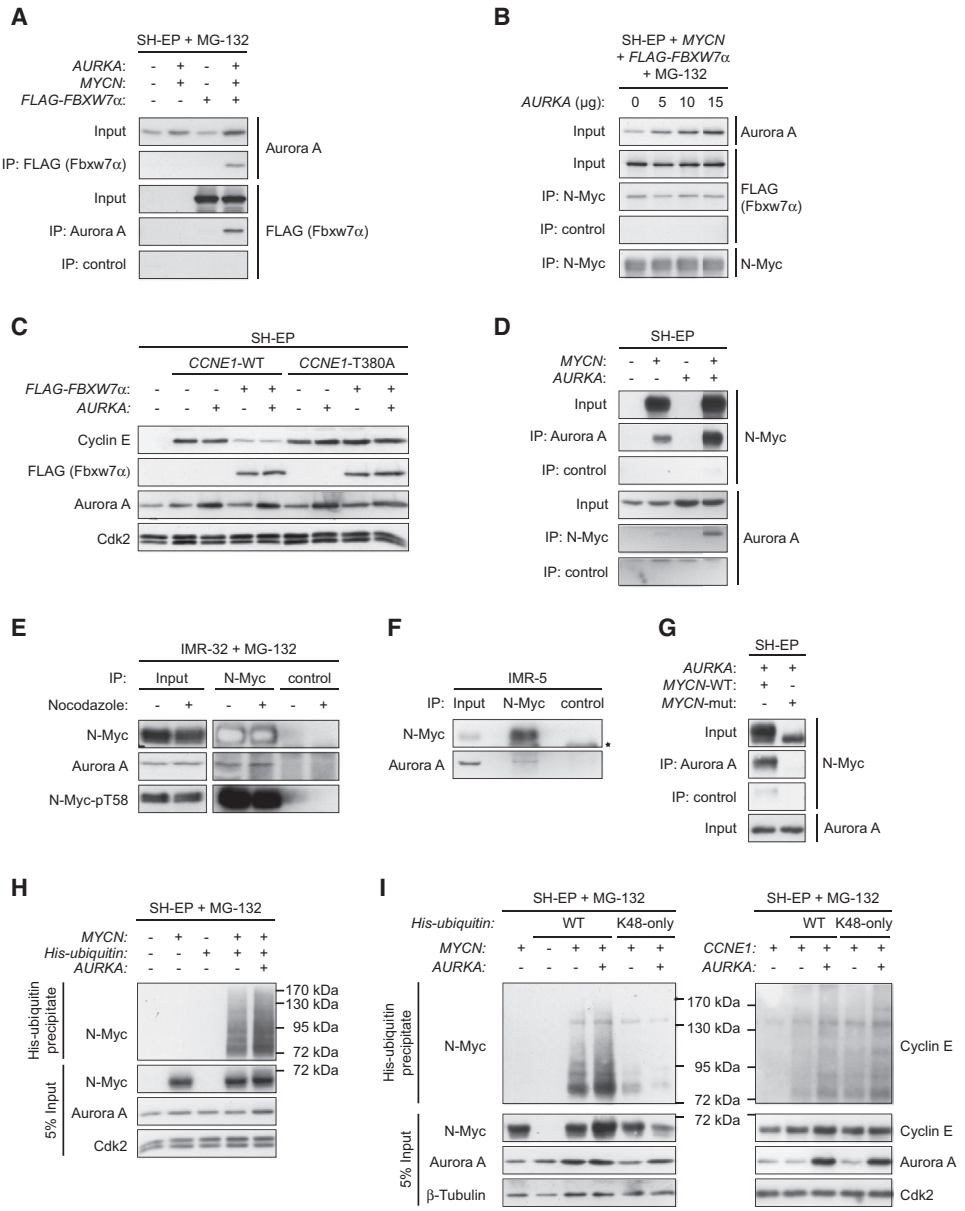

Figure 6. In Vivo Interactions of Aurora A with Fbxw7 and N-Myc

(A) Aurora A interacts with Fbxw7 in transfected cells. SH-EP cells were transfected with either control vectors or CMV-driven expression vectors encoding Aurora A and FLAG-tagged Fbxw7α as indicated. Lysates were prepared 48 hr after transfection and precipitated with Aurora A, FLAG, or control antibodies. Immunoblots of the input material (5% of the material used for precipitation) and of the immunoprecipitates are shown. MG-132 was added to the cells 6 hr before harvesting.

(B) Aurora A does not displace N-Myc from Fbxw7. SH-EP cells were transfected and harvested as before. Lysates were immunoprecipitated with N-Myc or control antibodies as indicated. MG-132 was added to the cells 12 hr before harvesting.

(C) Aurora A does not stabilize cyclin E. Immunoblots of SH-EP cells transfected with expression vectors encoding Aurora A, Fbxw7α, and either wild-type cyclin E or cyclin E(T380A), a mutant that is not recognized by Fbxw7 (Clurman et al., 1996), are shown. Lysates were prepared 48 hr after transfection.

(D) Aurora A interacts with N-Myc in transfected cells. The experiment was performed as before. Lysates were immunoprecipitated with Aurora A, N-Myc, or control antibodies as indicated. MG-132 was added to the cells 6 hr before harvesting.

(E) Interaction of endogenous N-Myc and Aurora A. IMR-32 cells were lysed and lysates were immunoprecipitated with antibodies directed against N-Myc or control antibodies. Immunoprecipitates were probed with antibodies directed against Aurora A, N-Myc, or antibodies that recognize N-Myc phosphorylated at T58 (N-Myc-pT58). Where indicated, nocodazole was added 18 hr before harvesting. MG-132 was added for 4 hr. The input lanes correspond to 2% of the material used for immunoprecipitations.

(F) Endogenous N-Myc and Aurora A interact in the absence of MG-132. The experiment was performed from lysates of IMR-5 cells as described in the legend to (E), except that neither MG-132 nor nocodazole was added to the cells. The asterisk denotes the heavy chain.

(G) Aurora A interacts with wild-type N-Myc, but not with N-Myc(T58A;S62A). SH-EP cells were transfected with the indicated expression vectors and analyzed as in (A). Input lanes show 2.5% of the material used for immunoprecipitation.

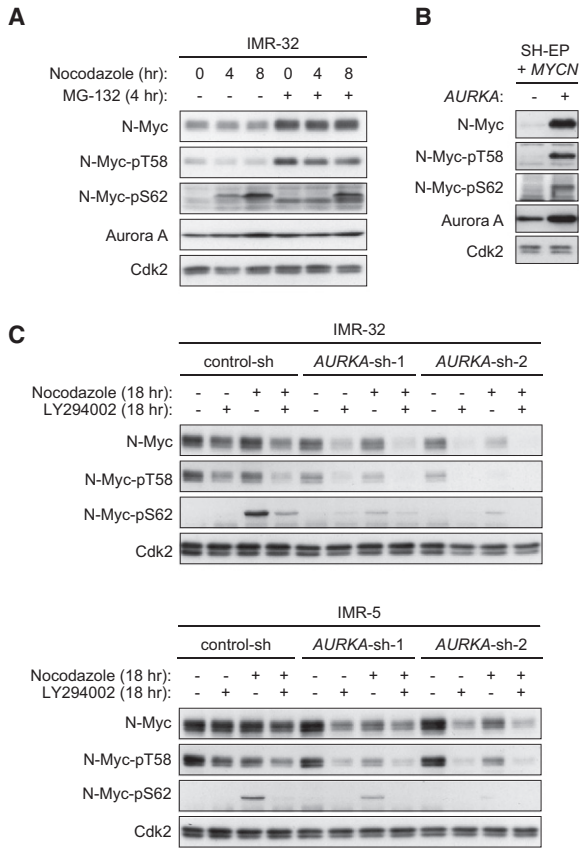

Figure 7. Aurora A Stabilizes Endogenous N-Myc during Mitosis and in the Absence of PI3-Kinase Activity

(A) Phosphorylation of S62 of N-Myc occurs in mitosis of *MYCN*-amplified neuroblastoma cells. IMR-32 cells were incubated with nocodazole and/or MG-132 as shown. At the indicated time points, cells were harvested and probed with antibodies against Aurora A, N-Myc, N-Myc-pT58, and N-Myc-pS62.

(B) Aurora A stabilizes N-Myc that is phosphorylated at T58 and S62. SH-EP cells were transfected with expression vectors encoding Aurora A and N-Myc as before and harvested after 48 hr. Lysates were probed with the indicated antibodies.

(C) Endogenous Aurora A stabilizes N-Myc in the absence of PI3-kinase and during mitosis in *MYCN*-amplified neuroblastoma cells. IMR-32 cells (upper panels) or IMR-5 cells (lower panels) were infected with retroviruses expressing either control shRNA or two different shRNA vectors targeting *AURKA*. Where indicated, pools of resistant cells were incubated with nocodazole, LY294002, or both for 18 hr. Lysates were prepared and probed with antibodies detecting total N-Myc, N-Myc phosphorylated at T58, or N-Myc phosphorylated at S62 as shown.

DISCUSSION

We report here that Aurora A has a critical function in stabilizing N-Myc in neuroblastomas that carry an amplified *MYCN* gene. In neuronal progenitor cells of the central nervous system, degradation of N-Myc is linked to progression through mitosis since it is initiated by phosphorylation at S62 by cyclin B/Cdk1 in prophase (Sjostrom et al., 2005). Phosphorylation at S62 serves as a priming site for Gsk3, which subsequently phosphorylates T58 to initiate Fbxw7-mediated degradation (Sjostrom et al., 2005). Gsk3 in turn is inhibited via phosphorylation by Akt. As a result, signaling via PI3-kinase and Akt stabilizes N-Myc and protects it from proteasomal degradation (Sjostrom et al., 2005). Since N-Myc is required for the proliferation of neuronal progenitors, the mitotic degradation of N-Myc that occurs in the absence of growth factor-dependent signals allows cell-cycle exit and commencement of differentiation (Knoepfler et al., 2002; Sjostrom et al., 2005). Consistent with this view, enforced expression of N-Myc, in particular of mutant alleles of N-Myc that cannot be phosphorylated by Gsk3, induces proliferation and suppresses differentiation of neuronal progenitor cells (Kenney et al., 2004).

In contrast to neuronal precursor cells, pharmacological inhibition of PI3-kinase coupled with cell-cycle arrest in mitosis had only moderate effects on N-Myc protein levels in *MYCN*-amplified neuroblastoma cells. We showed that this is due to elevated levels of Aurora A, which inhibit the mitotic degradation of N-Myc in such cells. Conversely, coexpression of Aurora A with N-Myc induces the accumulation of N-Myc that is phosphorylated at both S62 and T58. As a result, high levels of Aurora A effectively uncouple degradation of N-Myc from PI3-kinase-dependent signaling in neuroblastoma. We propose that elevated levels of Aurora A may inhibit the cell-cycle exit of neuroblasts during late embryonic and early postnatal development and thereby contribute to the genesis of neuroblastoma. Notably, the relationship of Aurora A and N-Myc in neuroblastoma has properties of a positive feedback loop: expression of *AURKA* is elevated in *MYCN*-amplified neuroblastoma and induced by activation of N-Myc in culture (Berwanger et al., 2002), and conversely, Aurora A stabilizes the N-Myc protein. Amplification of either gene might therefore lock this loop in an active state. Attempts to test this model by enforcing stable expression of Aurora A failed since retroviral expression of either wild-type or kinase-dead Aurora A suppressed colony formation in multiple cell lines, arguing that additional genetic events must occur that allow tumor cells to accommodate elevated levels of *AURKA*. A model summarizing our findings is shown in Figure 8.

Previous work has demonstrated that specific sequences in Myc proteins that are highly conserved in evolution (Mycboxes) are required for ubiquitination of Myc (Mycbox I, surrounding T58 and S62) and the subsequent degradation of ubiquitinated Myc (Mycbox III), arguing that both steps involve distinct mechanisms (Herbst et al., 2004). Aurora A inhibits the degradation of ubiquitinated N-Myc, similar to what is observed for deletion mutants lacking Mycbox III. Our finding that Aurora A also

(H) Aurora A induces the accumulation of ubiquitinated N-Myc. SH-EP cells were transfected with the indicated expression vectors. Cells were harvested 48 hr after transfection. Four hours before harvesting, MG-132 (25 μM) was added to block proteasomal degradation. Ubiquitinated proteins were recovered on Ni-NTA agarose and detected with N-Myc antibodies.

(I) Aurora A does not promote the accumulation of N-Myc carrying K48-linked polyubiquitin chains. Left panel: N-Myc ubiquitination assays were performed as above using either wild-type ubiquitin or ubiquitin in which all lysine residues except K48 were mutated to arginine (K48-only). Right panel: ubiquitination of cyclin E was used as a control to demonstrate that K48-only ubiquitin is not generally deficient in conjugation.

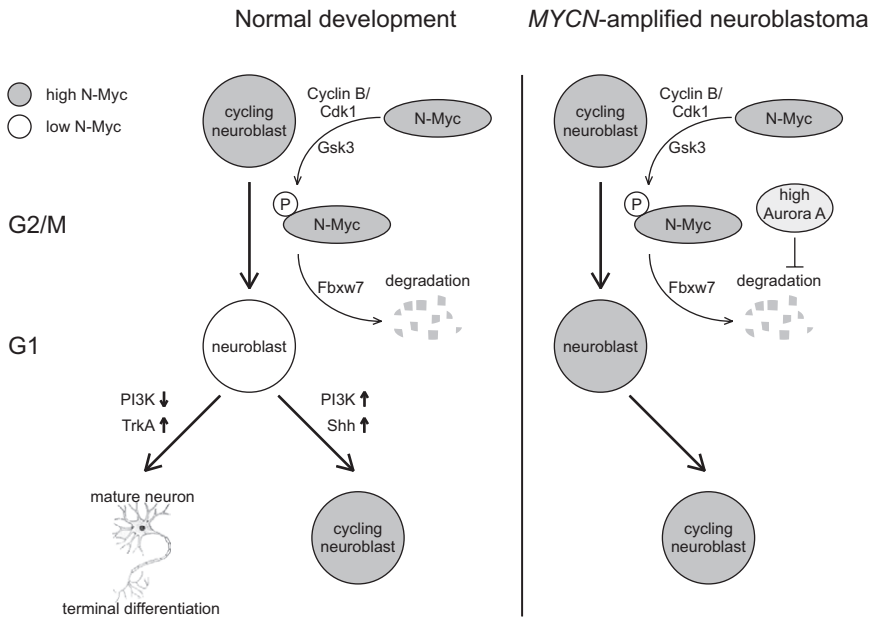

Figure 8. Model Summarizing Our Findings
The mitotic degradation of N-Myc has been proposed to couple growth factor-dependent signals to N-Myc levels at the start of the cell cycle and thereby allow cell-cycle exit of neuroblasts during the development of the nervous system (Sjostrom et al., 2005). We propose that high levels of Aurora A in *MYCN*-amplified neuroblastoma (either due to an amplification of the *AURKA* gene or due to activation of *AURKA* mRNA expression in response to the high N-Myc levels) uncouple this regulatory circuit and maintain neuroblastoma cells in a proliferative state independently of the presence of external growth factors.

stabilizes N-Myc in the presence of the spindle poison nocodazole argues against a simple sequestration of N-Myc from the proteasome at the spindle. Two possible mechanisms can account for our observations. First, binding of Aurora A to N-Myc might inhibit ubiquitination at individual lysine residues in N-Myc that are critical for degradation, and this effect may be missed by looking at total ubiquitination of N-Myc. An alternative explanation is supported by our observation that Aurora A requires the presence of K63 or K11 to promote the accumulation of ubiquitinated N-Myc. This suggests that Aurora A promotes the synthesis of non-K48-linked ubiquitin chains that do not support degradation (Kim et al., 2007). The specificity of chain linkage is dictated by a combination of ubiquitin ligase and the ubiquitin-conjugating enzyme (Ubc) that is used for ubiquitination (Kim et al., 2007): for example, Fbxw7 uses Cdc34 to synthesize K48-linked polyubiquitin chains to degrade Myc (N.P., unpublished data). Therefore, we propose that Aurora A recruits Ubcs that can conjugate to K11, K63, or both in addition to K48; one candidate is Ube2n, which directs the synthesis of K63-linked polyubiquitin chains and interacts with Aurora A (Ewart-Toland et al., 2003). At present, we have been unable to detect complexes of N-Myc, Aurora A, and Ube2n, so the precise role of Ube2n or other Ubcs in the stabilizing function of Aurora A remains to be determined. If factors that act in a manner similar to Aurora A also exist for c-Myc, this model may explain the recent observation that HectH9, a ubiquitin ligase that assembles the synthesis of predominantly K63-linked chains on c-Myc, assembles predominantly K48-linked chains on N-Myc (Adhikary et al., 2005; Zhao et al., 2008). Furthermore, ubiquitination of Myc by HectH9 or Skp2 stimulates the transcriptional activity of Myc in addition to regulating turnover; similarly, it is possible that Aurora A—via stabilizing ubiquitinated N-Myc—activates its function as a transcription factor (Adhikary et al., 2005; Kim et al., 2003).

AURKA is highly expressed relative to normal tissue and amplified in multiple human tumors (Zhou et al., 1998). Ectopic expression of *AURKA* transforms rodent fibroblasts in culture and induces hyperplasia and mammary tumors when expressed under the control of an MMTV promoter in transgenic mice (Bischoff et al., 1998; Wang et al., 2006). Together, these observations provide strong evidence for an oncogenic function of Aurora A in several human tumors.

Amplification of the *AURKA* gene has been taken as evidence that the kinase activity of Aurora A is under selective pressure during tumorigenesis, and, as a consequence, inhibitors of Aurora A kinase are being developed as anticancer therapeutics (Carvajal et al., 2006). In support of this approach, transformation of rodent fibroblasts by Aurora A depends on its kinase activity (Bischoff et al., 1998). Furthermore, the ability of Aurora A to enhance translation of c-Myc and prevent cellular senescence, which may be critical for its ability to transform rodent fibroblasts, depends on phosphorylation of cytoplasmic polyadenylation element binding protein (CPEB) (Groisman et al., 2006).

In contrast, Aurora A kinase activity is not required for stabilization of N-Myc or for the ability of Aurora A to induce centrosome duplication, suggesting that inhibition of Aurora A kinase may fail to inhibit critical oncogenic functions of Aurora A (Meraldi et al., 2002). Aurora A had no effect on the stability of cyclin E or c-Myc, other proteins that are degraded by Fbxw7, suggesting that the function of Aurora A described here contributes selectively to the development of N-Myc-dependent tumors. In addition to neuroblastoma, both N-Myc and Aurora A are also involved in the genesis of medulloblastoma (Neben et al., 2004). Similarly, both *MYCN* and *AURKA* are expressed at high levels in glioblastoma, astrocytoma, and prostate carcinoma, suggesting that stabilization of N-Myc by Aurora A may not be restricted to childhood tumors. Finally, both Aurora A and N-Myc have been implicated in the genesis of acute myelocytic leukemia (AML), arguing that stabilization of N-Myc may contribute to Aurora A-dependent tumorigenesis in several entities.

Notably, elevation of N-Myc levels may also contribute to tumor-relevant phenotypes, such as the ability to induce genomic instability and aneuploidy, that have been ascribed to the mitotic functions of Aurora A. For example, the mitotic checkpoint gene *MAD2L1* is a direct target of N-Myc (Berwanger et al., 2002), and enhanced expression of *MAD2L1* is oncogenic and

generates phenotypes that are reminiscent of *AURKA* overexpression (Sotillo et al., 2007). Taken together, our data suggest that deregulation of N-Myc may contribute significantly to the oncogenic properties of Aurora A.

EXPERIMENTAL PROCEDURES

Cell Culture and Patient Samples

Neuroblastoma cell lines stably expressing the murine ecotropic receptor with a hygromycin or neomycin resistance gene were grown in RPMI 1640 supplemented with 10% heat-inactivated fetal bovine serum and hygromycin (100 μg/ml) or G418 (200 μg/ml), respectively. Treatment with 4-hydroxytamoxifen (4-OHT; 200 nM), cycloheximide (50 μg/ml), MG-132 (5–25 μM), nocodazole (0.1 μg/ml), LY294002 (50 μM), and hesperadin (100 nM) was carried out as indicated. For colony assays, cells were fixed with 70% ethanol and stained with crystal violet. FACS analysis was performed using propidium iodide staining of ethanol-fixed cells, a FACSCalibur flow cytometer (BD Biosciences), and ModFit LT software.

Primary neuroblastoma samples were obtained from patients participating in the German Neuroblastoma Study, and informed consent was obtained within the German Neuroblastoma Study Group.

Plasmids, Transfection, and Retroviral Infection

shRNA-expressing vectors were based on the pSUPER.retro.puro plasmid and were either picked from a preexisting shRNA library (Berns et al., 2004) or cloned from oligonucleotides. *MYCN* and *AURKA* coding sequences were cloned into the BamHI or the BamHI and XhoI sites of pcDNA3, respectively. Expression vectors encoding the Fbxw7α and Fbxw7γ isoforms (p3x*FLAG-FBXW7-MYC*-CMV) and those encoding cyclin E1 wild-type and T380A mutant were obtained from B.E. Clurman (University of Washington, Seattle). Site-directed mutagenesis using the QuikChange XL Site-Directed Mutagenesis Kit (Stratagene) was performed to generate constructs expressing mutant *MYCN* or *AURKA*.

Cells were transiently transfected using the calcium phosphate method with varying amounts of DNA (2–30 μg). For retroviral transduction, the Phoenix-Eco helper cell line (American Type Culture Collection) was used. Control FACS analyses showed that less than 5% of cells underwent apoptosis under any experimental condition.

Microarray Experiments and qRT-PCR

Fluorescently labeled cDNA was prepared from 2 μg preamplified total RNA by oligo(dT)-primed synthesis using CyScript reverse transcriptase in the presence of aminoallyl-dUTP followed by incubation with either Cy3 or Cy5 NHS esters (Amersham CyScribe Post-Labeling Kit). Each experiment was performed as a sandwich hybridization using two arrays, and two independent arrays were performed in a flip-color design for each data point. Data from all four hybridizations were averaged for further statistical analysis.

For qRT-PCR, total RNA was transcribed into cDNA using random hexanucleotide primers and M-MLV reverse transcriptase. qRT-PCR was performed in triplicates with cDNA corresponding to 40 ng total RNA using ABsolute QPCR SYBR Green Mix (ABgene) on an Mx3000P system (Stratagene) at 60°C annealing temperature. Relative expression was calculated according to the ΔΔCt relative quantification method using *RPS14* as a calibrator, except where stated otherwise. Error bars represent standard deviation of triplicates.

Immunoblot and Immunoprecipitation

Whole-cell extracts were prepared using three rounds of freeze/thaw in buffer containing 50 mM Tris (pH 8), 150 mM NaCl, 1% NP-40, and a cocktail of phosphatase and protease inhibitors. Antibodies used are listed in the Supplemental Experimental Procedures.

For immunoprecipitation, lysis was carried out on ice in buffer containing 50 mM Tris (pH 7.5), 120 mM NaCl, 5 mM EDTA, 0.5% NP-40, and inhibitors (as above) followed by sonication. Coimmunoprecipitation was performed using 1 μg of antibodies and 150–300 μg lysate for exogenous proteins or 2–9 mg for endogenous proteins.

Kinase and Ubiquitination Assays

For immunocomplex in vitro kinase assay, 800 μg lysate was immunoprecipitated with Aurora A or control antibody, washed and equilibrated in kinase buffer (50 mM Tris [pH 7.4], 10 mM $MgCl_2$, 1 mM DTT, and phosphatase and protease inhibitors), incubated for 30 min at 30°C with 5 μCi [γ-^{32}P]ATP and 1.5 μg recombinant histone H3, separated on a 15% SDS polyacrylamide gel, dried, and subjected to autoradiography. Ubiquitination assays were performed as described in Adhikary et al. (2005).

ACCESSION NUMBERS

Microarray results described herein are accessible at ArrayExpress (http://www.ebi.ac.uk/microarray-as/ae/) under the accession number E-MEXP-1496.

SUPPLEMENTAL DATA

The Supplemental Data include Supplemental Experimental Procedures, one table, and eight figures and can be found with this article online at http://www.cancercell.org/supplemental/S1535-6108(08)00408-X.

ACKNOWLEDGMENTS

We thank B. Samans for analysis of microarray data of Aurora A-depleted cells, N. Kraut (Boehringer Ingelheim, Vienna) for hesperadin, A. Behrens (London Research Institute) for Fbxw7 antibody, and A. Eggert for providing critical materials. This study was supported by grants from the Association for International Cancer Research to B.B. and M.E., the Bundesministerium für Bildung und Forschung to H.C. and M.E., and the European Union ("INTACT") to R.B. and M.E.

Received: February 28, 2008
Revised: November 25, 2008
Accepted: December 8, 2008
Published: January 5, 2009

REFERENCES

Adhikary, S., Marinoni, F., Hock, A., Hulleman, E., Popov, N., Beier, R., Bernard, S., Quarto, M., Capra, M., Goettig, S., et al. (2005). The ubiquitin ligase HectH9 regulates transcriptional activation by Myc and is essential for tumor cell proliferation. Cell *123*, 409–421.

Arvanitis, C., and Felsher, D.W. (2006). Conditional transgenic models define how MYC initiates and maintains tumorigenesis. Semin. Cancer Biol. *16*, 313–317.

Berns, K., Hijmans, E.M., Mullenders, J., Brummelkamp, T.R., Velds, A., Heimerikx, M., Kerkhoven, R.M., Madiredjo, M., Nijkamp, W., Weigelt, B., et al. (2004). A large-scale RNAi screen in human cells identifies new components of the p53 pathway. Nature *428*, 431–437.

Berwanger, B., Hartmann, O., Bergmann, E., Nielsen, D., Krause, M., Kartal, A., Flynn, D., Wiedemeyer, R., Schwab, M., Schäfer, H., et al. (2002). Loss of a Fyn-regulated differentiation and growth arrest pathway in advanced stage neuroblastoma. Cancer Cell *2*, 377–386.

Bischoff, J.R., Anderson, L., Zhu, Y., Mossie, K., Ng, L., Souza, B., Schryver, B., Flanagan, P., Clairvoyant, F., Ginther, C., et al. (1998). A homologue of Drosophila aurora kinase is oncogenic and amplified in human colorectal cancers. EMBO J. *17*, 3052–3065.

Carvajal, R.D., Tse, A., and Schwartz, G.K. (2006). Aurora kinases: new targets for cancer therapy. Clin. Cancer Res. *12*, 6869–6875.

Clurman, B.E., Sheaff, R.J., Thress, K., Groudine, M., and Roberts, J.M. (1996). Turnover of cyclin E by the ubiquitin-proteasome pathway is regulated by cdk2 binding and cyclin phosphorylation. Genes Dev. *10*, 1979–1990.

Cross, D.A., Alessi, D.R., Cohen, P., Andjelkovich, M., and Hemmings, B.A. (1995). Inhibition of glycogen synthase kinase-3 by insulin mediated by protein kinase B. Nature *378*, 785–789.

Ewart-Toland, A., Briassouli, P., de Koning, J.P., Mao, J.H., Yuan, J., Chan, F., MacCarthy-Morrogh, L., Ponder, B.A., Nagase, H., Burn, J., et al. (2003). Identification of Stk6/STK15 as a candidate low-penetrance tumor-susceptibility gene in mouse and human. Nat. Genet. *34*, 403–412.

Fujii, Y., Yada, M., Nishiyama, M., Kamura, T., Takahashi, H., Tsunematsu, R., Susaki, E., Nakagawa, T., Matsumoto, A., and Nakayama, K.I. (2006). Fbxw7 contributes to tumor suppression by targeting multiple proteins for ubiquitin-dependent degradation. Cancer Sci. *97*, 729–736.

Galderisi, U., Di Bernardo, G., Cipollaro, M., Peluso, G., Cascino, A., Cotrufo, R., and Melone, M.A. (1999). Differentiation and apoptosis of neuroblastoma cells: role of N-myc gene product. J. Cell. Biochem. *73*, 97–105.

Gottlieb, E., Haffner, R., von Rüden, T., Wagner, E.F., and Oren, M. (1994). Down-regulation of wild-type p53 activity interferes with apoptosis of IL-3-dependent hematopoietic cells following IL-3 withdrawal. EMBO J *13*, 1368–1374.

Grimmer, M.R., and Weiss, W.A. (2006). Childhood tumors of the nervous system as disorders of normal development. Curr. Opin. Pediatr. *18*, 634–638.

Groisman, I., Ivshina, M., Marin, V., Kennedy, N.J., Davis, R.J., and Richter, J.D. (2006). Control of cellular senescence by CPEB. Genes Dev. *20*, 2701–2712.

Hauf, S., Cole, R.W., LaTerra, S., Zimmer, C., Schnapp, G., Walter, R., Heckel, A., van Meel, J., Rieder, C.L., and Peters, J.M. (2003). The small molecule Hesperadin reveals a role for Aurora B in correcting kinetochore-microtubule attachment and in maintaining the spindle assembly checkpoint. J. Cell Biol. *161*, 281–294.

Herbst, A., Salghetti, S.E., Kim, S.Y., and Tansey, W.P. (2004). Multiple cell-type-specific elements regulate Myc protein stability. Oncogene *23*, 3863–3871.

Hirota, T., Kunitoku, N., Sasayama, T., Marumoto, T., Zhang, D., Nitta, M., Hatakeyama, K., and Saya, H. (2003). Aurora A and an interacting activator, the LIM protein Ajuba, are required for mitotic commitment in human cells. Cell *114*, 585–598.

Kaelin, W.G., Jr. (2005). The concept of synthetic lethality in the context of anticancer therapy. Nat. Rev. Cancer *5*, 689–698.

Katayama, H., Sasai, K., Kawai, H., Yuan, Z.M., Bondaruk, J., Suzuki, F., Fujii, S., Arlinghaus, R.B., Czerniak, B.A., and Sen, S. (2004). Phosphorylation by aurora kinase A induces Mdm2-mediated destabilization and inhibition of p53. Nat. Genet. *36*, 55–62.

Kenney, A.M., Widlund, H.R., and Rowitch, D.H. (2004). Hedgehog and PI-3 kinase signaling converge on Nmyc1 to promote cell cycle progression in cerebellar neuronal precursors. Development *131*, 217–228.

Kim, H.T., Kim, K.P., Lledias, F., Kisselev, A.F., Scaglione, K.M., Skowyra, D., Gygi, S.P., and Goldberg, A.L. (2007). Certain pairs of ubiquitin-conjugating enzymes (E2s) and ubiquitin-protein ligases (E3s) synthesize nondegradable forked ubiquitin chains containing all possible isopeptide linkages. J. Biol. Chem. *282*, 17375–17386.

Kim, S.Y., Herbst, A., Tworkowski, K.A., Salghetti, S.E., and Tansey, W.P. (2003). Skp2 regulates myc protein stability and activity. Mol. Cell *11*, 1177–1188.

Knoepfler, P.S., Cheng, P.F., and Eisenman, R.N. (2002). N-myc is essential during neurogenesis for the rapid expansion of progenitor cell populations and the inhibition of neuronal differentiation. Genes Dev. *16*, 2699–2712.

Koepp, D.M., Schaefer, L.K., Ye, X., Keyomarsi, K., Chu, C., Harper, J.W., and Elledge, S.J. (2001). Phosphorylation-dependent ubiquitination of cyclin E by the SCFFbw7 ubiquitin ligase. Science *294*, 173–177.

Meraldi, P., Honda, R., and Nigg, E.A. (2002). Aurora A overexpression reveals tetraploidization as a major route to centrosome amplification in p53−/− cells. EMBO J. *21*, 483–492.

Neben, K., Korshunov, A., Benner, A., Wrobel, G., Hahn, M., Kokocinski, F., Golanov, A., Joos, S., and Lichter, P. (2004). Microarray-based screening for molecular markers in medulloblastoma revealed STK15 as independent predictor for survival. Cancer Res. *64*, 3103–3111.

Nilsson, J.A., Keller, U.B., Baudino, T.A., Yang, C., Norton, S., Old, J.A., Nilsson, L.M., Neale, G., Kramer, D.L., Porter, C.W., and Cleveland, J.L. (2005). Targeting ornithine decarboxylase in Myc-induced lymphomagenesis prevents tumor formation. Cancer Cell *7*, 433–444.

Schulte, J.H., Horn, S., Otto, T., Samans, B., Heukamp, L.C., Eilers, U.C., Krause, M., Astrahantseff, K., Klein-Hitpass, L., Buettner, R., et al. (2008). MYCN regulates oncogenic MicroRNAs in neuroblastoma. Int. J. Cancer *122*, 699–704.

Sjostrom, S.K., Finn, G., Hahn, W.C., Rowitch, D.H., and Kenney, A.M. (2005). The Cdk1 complex plays a prime role in regulating N-myc phosphorylation and turnover in neural precursors. Dev. Cell *9*, 327–338.

Sotillo, R., Hernando, E., Diaz-Rodriguez, E., Teruya-Feldstein, J., Cordon-Cardo, C., Lowe, S.W., and Benezra, R. (2007). Mad2 overexpression promotes aneuploidy and tumorigenesis in mice. Cancer Cell *11*, 9–23.

Subramanian, A., Tamayo, P., Mootha, V.K., Mukherjee, S., Ebert, B.L., Gillette, M.A., Paulovich, A., Pomeroy, S.L., Golub, T.R., Lander, E.S., and Mesirov, J.P. (2005). Gene set enrichment analysis: a knowledge-based approach for interpreting genome-wide expression profiles. Proc. Natl. Acad. Sci. USA *102*, 15545–15550.

Valsesia-Wittmann, S., Magdeleine, M., Dupasquier, S., Garin, E., Jallas, A.C., Combaret, V., Krause, A., Leissner, P., and Puisieux, A. (2004). Oncogenic cooperation between H-Twist and N-Myc overrides failsafe programs in cancer cells. Cancer Cell *6*, 625–630.

Wang, X., Zhou, Y.X., Qiao, W., Tominaga, Y., Ouchi, M., Ouchi, T., and Deng, C.X. (2006). Overexpression of aurora kinase A in mouse mammary epithelium induces genetic instability preceding mammary tumor formation. Oncogene *25*, 7148–7158.

Welcker, M., Orian, A., Grim, J.A., Eisenman, R.N., and Clurman, B.E. (2004). A nucleolar isoform of the Fbw7 ubiquitin ligase regulates c-Myc and cell size. Curr. Biol. *14*, 1852–1857.

Westermann, F., and Schwab, M. (2002). Genetic parameters of neuroblastomas. Cancer Lett. *184*, 127–147.

Yada, M., Hatakeyama, S., Kamura, T., Nishiyama, M., Tsunematsu, R., Imaki, H., Ishida, N., Okumura, F., Nakayama, K., and Nakayama, K.I. (2004). Phosphorylation-dependent degradation of c-Myc is mediated by the F-box protein Fbw7. EMBO J. *23*, 2116–2125.

Zhao, X., Heng, J.I., Guardavaccaro, D., Jiang, R., Pagano, M., Guillemot, F., Iavarone, A., and Lasorella, A. (2008). The HECT-domain ubiquitin ligase Huwe1 controls neural differentiation and proliferation by destabilizing the N-Myc oncoprotein. Nat. Cell Biol. *10*, 643–653.

Zhou, H., Kuang, J., Zhong, L., Kuo, W.L., Gray, J.W., Sahin, A., Brinkley, B.R., and Sen, S. (1998). Tumour amplified kinase STK15/BTAK induces centrosome amplification, aneuploidy and transformation. Nat. Genet. *20*, 189–193.